Strong Electromechanical Coupling of an Atomic Force Microscope Cantilever to a Quantum Dot

Steven D. Bennett, Lynda Cockins, Yoichi Miyahara, Peter Grütter, and Aashish A. Clerk

Department of Physics, McGill University, Montreal, Quebec, Canada H3A 2T8

(Received 6 October 2009; published 8 January 2010)

We present theoretical and experimental results on the mechanical damping of an atomic force microscope cantilever strongly coupled to a self-assembled InAs quantum dot. When the cantilever oscillation amplitude is large, its motion dominates the charge dynamics of the dot which in turn leads to nonlinear, amplitude-dependent damping of the cantilever. We observe highly asymmetric line shapes of Coulomb blockade peaks in the damping that reflect the degeneracy of energy levels on the dot. Furthermore, we predict that excited state spectroscopy is possible by studying the damping versus oscillation amplitude, in analogy with varying the amplitude of an ac gate voltage.

DOI: 10.1103/PhysRevLett.104.017203 PACS numbers: 85.85.+j, 73.22.−f, 85.35.Gv

Coupling a mechanical object to quantum electronics is a means to probe both the mechanics and the electronics with extreme sensitivity. It has been predicted that the electronics may be used to measure the quantum nature of the mechanical object [1], and the reverse—using mechanics to measure quantum effects in mesoscopic electronics—was recently demonstrated with superconducting qubits [2]. Electromechanical systems that have attracted considerable attention recently include quantum shuttles [3], and mechanics coupled to single electron transistors (SETs) [4,5] or tunnel junctions [6,7]. In most systems studied, the interaction between the electronic and mechanical components is weak.

In this Letter we study strong coupling effects, both theoretically and experimentally, in an electromechanical system consisting of a quantum dot capacitively coupled to an atomic force microscope (AFM) cantilever. Electrons tunneling on and off the dot effectively damp the cantilever, and this damping exhibits Coulomb blockade peaks as a function of applied voltage similar to those well known in the dot conductance [8–10]. It has long been predicted that level degeneracy on the dot leads to line shape asymmetry of Coulomb blockade peaks in the conductance [11]. Recently, we observed corresponding temperature-dependent peak shifts in the damping at weak coupling [10], but the line shape asymmetry was far too small to be measured. However, by driving the cantilever to large oscillation amplitudes we enter a regime of strong coupling: within one period, the cantilever motion is large enough to swing the dot completely on or off of a charge degeneracy point. This leads to a dramatic enhancement of the line shape asymmetry that is much greater than expected from simply extrapolating the weak coupling theory; it is a nonadiabatic effect that stems from the similar time scales for dynamics of the cantilever and the dot. Furthermore, we predict that by measuring the damping versus applied voltage and oscillation amplitude, strong coupling provides a way to perform excited state spectroscopy on the dot. Note that very different strong coupling effects unrelated to degeneracy were recently reported for a driven carbon nanotube coupled to an embedded dot [12,13].

Our results show that an AFM operated at large oscillation amplitudes may be used to study degeneracy and level spacing, so-called shell structure, in confined electronic systems. The particular systems studied here, self-assembled quantum dots, are candidates for applications such as quantum information processing, and measuring their shell structure has attracted extensive research effort [14–17]. Our technique allows the level degeneracy to be read off from a single sweep of damping versus applied voltage, and offers the practical advantage of being able to address many dots one by one without the need for electrical contacts.

Setup.—The mechanical oscillator is an AFM cantilever with resonant frequency $\omega_0/2\pi = 166$ kHz, spring constant $k_0 = 48$ N/m, and intrinsic quality factor of typically $Q_0 \sim 2 \times 10^5$. It is driven on resonance in self-oscillation mode at constant amplitude and mean tip-sample gap of 19 nm [10]. The cantilever is coated with a 10 nm Ti adhesion layer and a 20 nm Pt layer to ensure good electrical conductivity at low temperature. All data in this Letter were collected at 5 K. The sample is grown by chemical beam epitaxy, with the relevant features being uncapped InAs dots on top of a 20 nm InP tunnel barrier and a 10 nm InGaAs two-dimensional electron gas (2DEG)

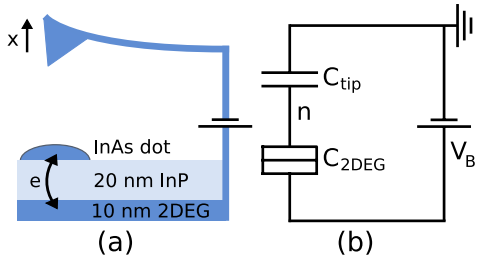

FIG. 1 (color online). (a) Schematic of the setup. (b) Equivalent circuit diagram, where C_{tip} depends on x.

which acts as a back electrode. For full sample details, see Ref. [10]. The voltage V_B is applied to the 2DEG layer, with the cantilever electrically grounded (see Fig. 1). The potential drop between the 2DEG and the dot is αV_B, where $\alpha = C_{\rm tip}/C_\Sigma$ is extracted from the experiment and $C_\Sigma = C_{\rm tip} + C_{\rm 2DEG}$ is the total dot capacitance. The dot-cantilever coupling arises through $C_{\rm tip}$, which depends on the tip position x. Electrons tunnel between the 2DEG and the dot when V_B is sufficient to lift Coulomb blockade, while tunneling between the dot and tip is negligible due to the much larger tunnel barrier height of the vacuum gap. The fluctuating charge on the dot results in both damping and a resonance frequency shift $\Delta\omega$ of the cantilever; in the limit of weak coupling these are well described by linear response [18]. Here we focus on the damping, which is provided in addition to the frequency shift by a phase-locked loop frequency detector and automatic gain controller [10].

Model.—For small cantilever motion compared to the tip-dot separation, $C_{\rm tip}$ is linear in x and we can write the charging Hamiltonian of the dot as [19]

$$\mathcal{H}_C = E_C[(n-\mathcal{N})^2 - (1 + C_{\rm 2DEG}/C_{\rm tip})\mathcal{N}^2] \simeq \mathcal{H}_{C,0} + \Delta\mathcal{H}_{\rm osc} - Anx, \quad (1)$$

where n is the number of electrons on the dot, $\mathcal{N} = -V_B C_{\rm tip}/e$ is the dimensionless gate voltage, and $E_C = e^2/2C_\Sigma$ is the charging energy [20]. $\mathcal{H}_{C,0}$ is the oscillator-independent part of $\mathcal{H}_C$, and $\Delta\mathcal{H}_{\rm osc}$ modifies the oscillator potential. The last term describes dot-cantilever coupling with strength $A = -(2E_C V_B/e)(1-\alpha)\partial C_{\rm tip}/\partial x$; from this term we see that the dot charge exerts a force An on the oscillator.

We focus on the voltage range where 0 or 1 extra electrons reside on the dot with other charge states prohibited by Coulomb blockade; it is simple to generalize this to n or $n+1$. The tunneling rates are calculated using Fermi's golden rule and accounting for the degeneracy of single particle levels on the dot. For a shell of degeneracy ν occupied by $n_{\rm shell}$ electrons, there are $\eta_+ = \nu - n_{\rm shell}$ ways to add an electron, and once it has been added there are $\eta_- = n_{\rm shell} + 1$ ways to remove it. The extra energy with 1 electron on the dot is $E(x) = 2E_C(1/2 - \mathcal{N}) - Ax$. In the classical oscillator limit, $\hbar\omega_0 \ll k_B T$ [21,22], this results in x-dependent rates Γ_+ (Γ_-) to add (remove) an electron,

$$\Gamma_\pm(x) = \eta_\pm \Gamma f[\pm E(x)], \quad (2)$$

where Γ is the tunneling rate to a single particle state and f is the Fermi function. The asymmetry between adding and removing electrons is the root of the asymmetry in Coulomb blockade peaks [11].

We describe the coupled system using a master equation for the charge on the dot combined with a Fokker-Planck equation for the phase space distribution of the oscillator [23,24]. The probabilities $P_0(x,u)$ and $P_1(x,u)$ to find the oscillator at position x and velocity u with 0 or 1 electrons on the dot satisfy master equations,

$$\partial_t P_0(x,u) = \mathcal{L}_0 P_0 + \Gamma_-(x)P_1 - \Gamma_+(x)P_0, \quad (3)$$

$$\partial_t P_1(x,u) = \mathcal{L}_1 P_1 + \Gamma_+(x)P_0 - \Gamma_-(x)P_1, \quad (4)$$

where $\mathcal{L}_n = \omega_0^2(x - x_n - \mathcal{F}/k_0)\partial_u - u\partial_x + \gamma_0\partial_u u$ describes a driven, damped harmonic oscillator and $x_n = An/k_0$ is the equilibrium position with n electrons on the dot. The damping γ_0 is intrinsic to the oscillator without coupling to the dot, and $\mathcal{F}$ is the external driving force.

While it is straightforward to simulate the master equations directly, we gain further insight by focusing on the simpler dynamics of system averages. Following Ref. [25], we make the approximation that averages of products may be factorized, justified by comparison with full simulations, and use Eqs. (3) and (4) to obtain coupled equations for the average quantities,

$$\partial_t\langle x\rangle = \langle u\rangle, \quad (5)$$

$$\partial_t\langle u\rangle = \omega_0^2\left(\frac{\mathcal{F} + A\langle P_1\rangle}{k_0} - \langle x\rangle\right) - \gamma_0\langle u\rangle, \quad (6)$$

$$\partial_t\langle P_1\rangle = \Gamma_+(\langle x\rangle)\langle P_0\rangle - \Gamma_-(\langle x\rangle)\langle P_1\rangle. \quad (7)$$

We seek a solution where the cantilever oscillates at constant amplitude a, as in experiment, such that $\langle x(t)\rangle = a\cos(\omega_0 t)$. Ignoring the frequency shift due to tunneling (since $\Delta\omega \ll \omega_0$) and assuming that the total damping is small ($\gamma_0 + \gamma_1 \ll \omega_0$, justified self-consistently), we find

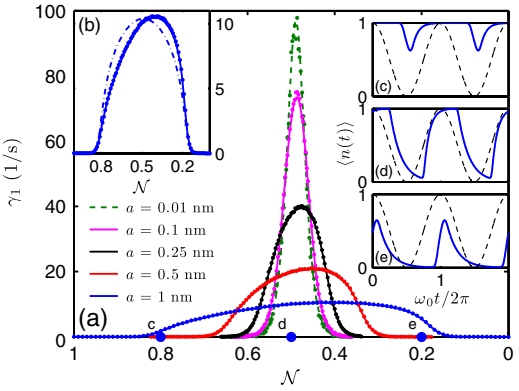

FIG. 2 (color online). (a) First damping peak calculated from simulation (dots) and semianalytic theory (solid lines). The green dashed line is from linear response. $\mathcal{N}$ is plotted in reverse for consistency with experiment. (b) Adiabatic approximation (dash-dotted), semianalytic theory (solid), and simulation (dots) for oscillation amplitude $a = 1$ nm. (c)–(e) Average dot charge versus time (solid) for $a = 1$ nm, at voltages marked in (a). Cantilever position is also shown (thin dashed) as a reference. We took $2E_C = 31$ meV, $\omega_0/\Gamma = 1$, and $A = 10$ meV/nm. Other parameters were taken from the experiment (see setup).

that the effective, amplitude-dependent damping due to tunneling is given by [25]

$$\gamma_1 = \frac{\omega_0^2 A}{\pi k_0 a} \int_0^{2\pi/\omega_0} dt \sin(\omega_0 t)\langle P_1(t)\rangle, \tag{8}$$

and obtain constant amplitude oscillations for $\mathcal{F} = -ak_0/\omega_0(\gamma_0 + \gamma_1)\sin(\omega_0 t)$. Equation (8) connects the damping to the out-of-phase part of the average dot charge, $\langle n(t)\rangle = \langle P_1(t)\rangle$, with respect to $\langle x(t)\rangle$. Note that the fluctuating dot charge causes damping even at weak coupling, and this is measurable using a sufficiently high quality oscillator [10], but Eq. (8) remains valid at strong coupling. It also reduces our calculation of γ_1 to solving Eq. (7) for $\langle P_1(t)\rangle$ numerically, a much easier task than directly simulating Eqs. (3) and (4).

Coulomb blockade peaks occur in the damping versus applied voltage at charge degeneracy points, where the dot energy is equal with either 0 or 1 electrons and charge fluctuations are maximal [10]. Figure 2(a) shows the first damping peak for several oscillation amplitudes, calculated from Eq. (8) and from direct simulation of Eqs. (3) and (4) following Ref. [24]. We assume the level structure of a cylindrical dot, with a twofold degenerate s shell and a fourfold degenerate p shell. The simulated damping is well described by linear response (green dashed) at weak coupling; note that even this peak is slightly asymmetric as expected. As the oscillation amplitude is increased, the peak becomes broadened and highly asymmetric. Note that the line shape at strong coupling is completely missed by an adiabatic approximation, where one assumes that the oscillator motion is much slower than tunneling [see Fig. 2(b)]. On the other hand, our semianalytic theory [i.e., Eq. (8)] agrees very well with the full simulation, so we use it to understand why the line shape is so highly asymmetric at strong coupling.

Asymmetric line shape.—The asymmetric line shape of Coulomb blockade peaks is a result of the asymmetry between adding or removing electrons to or from a degenerate shell on the dot [see Eq. (2)]. Consider the voltage points c and e on either side of the peak in Fig. 2(a), equal distances from its center such that the largest amplitude motion (broadest peak) swings $\mathcal{N}$ onto the charge degeneracy point. A tunneling event near $\mathcal{N} = 1/2$ is twice as likely to occur when starting from point e, where the dot is initially empty. This is because the rate to tunnel onto the dot when $\mathcal{N} = 1/2$ is $\Gamma_+ \sim 2\Gamma f(0) = \Gamma$ (for the first peak in the twofold degenerate s shell), while the rate to tunnel off is only $\Gamma_- \sim \Gamma[1 - f(0)] = \Gamma/2$. This asymmetry is apparent in the time dependence of $\langle n(t)\rangle$ at three voltage points, shown in Figs. 2(c)–2(e). Tunneling is more likely starting from point e, and this leads to increased damping. The situation is reversed in the second peak where there is only one way to add an electron to the half full s shell, but two ways to remove one once it is full. Thus the line shape asymmetry is a way to read off the shell degeneracy from a single V_B sweep: each peak is skewed away from the center of its shell.

While a similar argument leads to a very slightly asymmetric line shape at weak coupling, the asymmetry at strong coupling is *much greater* than one obtains by extending the weak coupling result to large oscillation amplitudes [see Fig. 2(b)]. For sufficiently strong coupling A, the change in gate voltage due to the oscillator motion dominates over the thermal broadening from the Fermi distribution of electrons in the back electrode, i.e., $Aa \geq k_B T$. Thus the harmonic distribution of the oscillator position $P(x)$, peaked at the turning points of its motion, causes the most asymmetric tunneling rates, $\Gamma_\pm(\pm a)$ at the oscillator extrema, to become especially important and dramatically increases the line shape asymmetry.

Here we point out the importance of relative time scales. For a slow oscillator, $\omega_0 \ll \Gamma$, the adiabatic approximation is valid since the dot charge quickly equilibrates in response to the slow cantilever motion. In this case the damping is simply given by a weighted average of the linear response result taken over the oscillating gate voltage, and the line shape asymmetry remains immeasurably small [see Fig. 2(b)]. In the opposite limit, $\omega_0 \gg \Gamma$, the dot charge cannot respond to the rapid oscillator motion and damping is suppressed. This is seen from Eq. (8): $\langle P_1(t)\rangle$ is roughly constant over one period of a fast oscillator and the dot-induced damping becomes vanishingly small. We study the regime $\omega_0 \sim \Gamma$, where the interplay between the two time scales leads to maximal and highly asymmetric damping.

Measured damping.—The experimentally measured cantilever damping is compared with theory in Fig. 3. In (a) and (b) we fit the first two Coulomb blockade peaks for three oscillation amplitudes using Eq. (8). For each peak, we used a single fit parameter A to fit the damping at all three amplitudes, obtaining the values given in the caption,

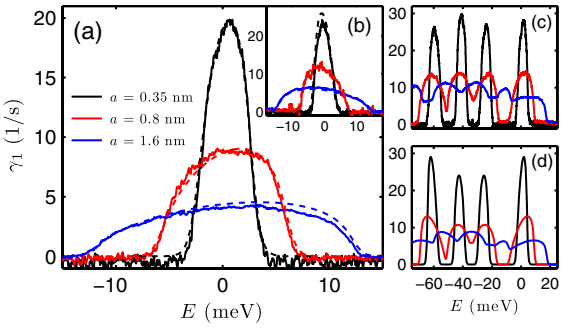

FIG. 3 (color online). (a) Experiment (solid) and theory (dashed) for the first damping peak. We converted eV_B to E using $\alpha = 0.04$ extracted at weak coupling. One fit value $A = 7.8$ meV/nm produced the theory curves for all three amplitudes. (b) Second peak with $A = 9.2$ meV/nm. (c) Measured damping over the p shell; theory shown in (d) with $A = 11$ meV/nm. Other parameters were taken from experiment as described in the text.

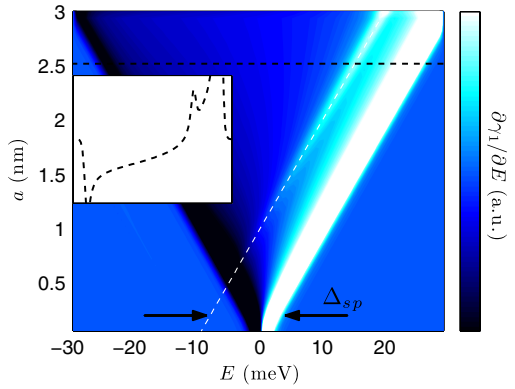

FIG. 4 (color online). Differential damping versus applied voltage (converted to E), and oscillation amplitude a. For large amplitudes, a peak appears on the line $E = Aa - \Delta_{sp}$ (white dashed line). Inset: cut along black dashed line. Parameters are the same as in Fig. 2.

in good agreement with those obtained at weak coupling on the same dot. We took $2E_C = 31$ meV, $\alpha = 0.04$, and $\Gamma = 70, 90$ kHz for peaks 1, 2; these values were extracted at weak coupling, with the rates Γ obtained from the on-peak ratio $\Delta\omega/\gamma_1$ [10]. Note that in our system, the damping is dominated by tunneling for voltages near a charge degeneracy point, where we find up to $\gamma_1/\gamma_0 \sim 20$ for small oscillations. This compares well with $\gamma_1/\gamma_0 \sim 50$ for SETs [5], 35 for nanotubes [12], and 1 for previous AFM experiments [8,9].

In Figs. 3(c) and 3(d) we show the measured and theoretical damping versus applied voltage over the entire p shell. This is calculated by extending our derivation of Eq. (8) to allow up to four electrons to occupy the fourfold degenerate p shell. We find qualitative agreement even in the crude approximation of constant E_C, and using single values of A and Γ over the entire shell [26]. We took $2E_C = 20$ meV for the p shell (estimated from the peak spacing), and roughly aligned the peaks by adjusting the p shell level splitting phenomenologically. Once this was done, a single set of parameters was used to produce the damping spectra at all three amplitudes. Most importantly, in both theory and experiment the four peaks in the p shell become five at large amplitudes, with peaks emerging between the charge degeneracy points. This is consistent with our theory above: at large amplitudes, the oscillator distribution $P(x)$ overwhelms temperature and makes the tunneling rates at its extrema most important. Thus, at very large amplitudes where $Aa = E_C$, tunneling is maximal when the applied voltage is at the midpoint between two degeneracy points.

Excited state spectroscopy.—Theoretically, our setup can be used to do excited state spectroscopy on the dot, since the oscillator is directly analogous to an ac gate voltage [27]. When the oscillator motion is large enough to allow tunneling to excited states, the damping increases. This occurs when the change in energy due to the oscillator is equal to the energy spacing, or $Aa \geq \Delta_{sp}$. At large amplitudes we expect a jump in γ_1 at the applied voltage where $E = Aa - \Delta_{sp}$, and a peak in $\partial\gamma_1/\partial E$. This defines a line versus E and a, shown in Fig. 4. Measuring the slope and intercept of this line in experiment would directly provide A and Δ_{sp}.

Conclusions.—We have demonstrated that oscillation amplitude is a useful new axis to exploit in using AFMs to probe quantum electronic systems. The implications extend beyond quantum dots to other confined electronic systems that can be placed on an insulating surface with a back electrode. In particular, we envision using an AFM to measure the level structure of single molecules.

This work was supported by NSERC, FQRNT, and CIFAR.

[1] A. D. Armour, M. P. Blencowe, and K. C. Schwab, Phys. Rev. Lett. **88**, 148301 (2002).
[2] M. D. LaHaye *et al.*, Nature (London) **459**, 960 (2009).
[3] D. R. Koenig, E. M. Weig, and J. P. Kotthaus, Nature Nanotech. **3**, 482 (2008).
[4] R. G. Knobel and A. N. Cleland, Nature (London) **424**, 291 (2003).
[5] A. Naik *et al.*, Nature (London) **443**, 193 (2006).
[6] N. E. Flowers-Jacobs, D. R. Schmidt, and K. W. Lehnert, Phys. Rev. Lett. **98**, 096804 (2007).
[7] M. Poggio *et al.*, Nature Phys. **4**, 635 (2008).
[8] M. T. Woodside and P. L. McEuen, Science **296**, 1098 (2002).
[9] J. Zhu, M. Brink, and P. L. McEuen, Nano Lett. **8**, 2399 (2008).
[10] L. Cockins *et al.*, arXiv:0910.0005.
[11] C. W. J. Beenakker, Phys. Rev. B **44**, 1646 (1991).
[12] G. A. Steele *et al.*, Science **325**, 1103 (2009).
[13] B. Lassagne *et al.*, Science **325**, 1107 (2009).
[14] H. Drexler *et al.*, Phys. Rev. Lett. **73**, 2252 (1994).
[15] B. T. Miller *et al.*, Phys. Rev. B **56**, 6764 (1997).
[16] S. Raymond *et al.*, Phys. Rev. Lett. **92**, 187402 (2004).
[17] M. Jung *et al.*, Appl. Phys. Lett. **87**, 203109 (2005).
[18] A. A. Clerk and S. Bennett, New J. Phys. **7**, 238 (2005).
[19] R. Stomp *et al.*, Phys. Rev. Lett. **94**, 056802 (2005).
[20] We neglect the term coupling x to n^2 since it is higher order in $\alpha \ll 1$.
[21] Quantum corrections to the rates occur when $\hbar\omega_0 \sim E$, $k_B T$ (see Ref. [22]), but these are negligible here.
[22] A. A. Clerk and S. M. Girvin, Phys. Rev. B **70**, 121303(R) (2004).
[23] A. D. Armour, M. P. Blencowe, and Y. Zhang, Phys. Rev. B **69**, 125313 (2004).
[24] C. B. Doiron, W. Belzig, and C. Bruder, Phys. Rev. B **74**, 205336 (2006).
[25] D. A. Rodrigues *et al.*, New J. Phys. **9**, 84 (2007).
[26] Both A and Γ are voltage dependent over the large voltage range of the p shell.
[27] J. M. Elzerman *et al.*, Appl. Phys. Lett. **84**, 4617 (2004).